MOLECULAR ECOLOGY

Molecular Ecology (2012) **21**, 1360–1378 doi: 10.1111/j.1365-294X.2012.05476.x

Urban landscape genetics: canopy cover predicts gene flow between white-footed mouse (*Peromyscus leucopus*) populations in New York City

JASON MUNSHI-SOUTH*†

*Department of Natural Sciences, A-0506, Baruch College, City University of New York (CUNY), 17 Lexington Avenue, New York, NY 10010, USA, †Ph.D. Program in Ecology, Evolutionary Biology, & Behavior, The Graduate Center, City University of New York, 365 Fifth Avenue, New York, NY 10016, USA

Abstract

In this study, I examine the influence of urban canopy cover on gene flow between 15 white-footed mouse (*Peromyscus leucopus*) populations in New York City parklands. Parks in the urban core are often highly fragmented, leading to rapid genetic differentiation of relatively nonvagile species. However, a diverse array of 'green' spaces may provide dispersal corridors through 'grey' urban infrastructure. I identify urban landscape features that promote genetic connectivity in an urban environment and compare the success of two different landscape connectivity approaches at explaining gene flow. Gene flow was associated with 'effective distances' between populations that were calculated based on per cent tree canopy cover using two different approaches: (i) isolation by effective distance (IED) that calculates the single best pathway to minimize passage through high-resistance (i.e. low canopy cover) areas, and (ii) isolation by resistance (IBR), an implementation of circuit theory that identifies all low-resistance paths through the landscape. IBR, but not IED, models were significantly associated with three measures of gene flow (*Nm* from F_{ST}, BayesAss+ and Migrate-*n*) after factoring out the influence of isolation by distance using partial Mantel tests. Predicted corridors for gene flow between city parks were largely narrow, linear parklands or vegetated spaces that are not managed for wildlife, such as cemeteries and roadway medians. These results have implications for understanding the impacts of urbanization trends on native wildlife, as well as for urban reforestation efforts that aim to improve urban ecosystem processes.

Keywords: circuit theory, gene flow, genetic differentiation, isolation by distance, least-cost path, migration

Received 25 June 2011; revision received 19 December 2011; accepted 2 January 2012

Introduction

Dispersal and gene flow are crucial parameters for understanding microevolution in fragmented populations (Keyghobadi 2007). Recording actual dispersal events is notoriously difficult for many species, but available data indicate that dispersal ability is correlated with population genetic differentiation (Bohonak 1999). Estimation of effective dispersal, that is, gene flow or migration resulting from dispersal followed by successful reproduction, has greatly improved because of recent analytical advances in estimating both contemporary and longer-term migration rates (Pearse & Crandall 2004; Waples & Gaggiotti 2006). Maintaining migration between fragmented populations is a key goal of conservation genetics (Frankham 2010), as reduced or absent migration is implicated in loss of biodiversity (Fahrig 2003), population differentiation (Mech & Hallett 2001) and reduced adaptive potential (Garant *et al.* 2007). Migration estimates from genetic markers can elucidate the mechanisms of genetic differentiation

Correspondence: Jason Munshi-South, Fax: +1 646 660 6201; E-mail: jason.munshi-south@baruch.cuny.edu

between animal groups and aid future efforts to restore connectivity to fragmented landscapes.

Island or stepping-stone models and summary statistics, such as F_{ST}, have typically been used to examine the impacts of migration on neutral genetic variation (Varvio *et al.* 1986; Gaines *et al.* 1997). Isolation-by-distance (IBD) approaches have also provided considerable support for the hypotheses of reduced migration and enhanced genetic differentiation with increasing Euclidean distance between populations (Jenkins *et al.* 2010). However, real organisms and their genes rarely follow the strict linear paths assumed by the above models. The composition and spatial configuration of landscape characteristics affect routes of movement, resulting in 'effective isolation' between occupied patches that may deviate from straight-line estimates (Ricketts 2001). One current focus of the discipline of landscape genetics is to understand how this effective isolation influences the genetic structuring of populations (Manel *et al.* 2003; Holderegger & Wagner 2008). Development of multiple approaches to infer the influence of landscape elements on population genetics has contributed to the rapid adoption of landscape genetics approaches in ecology and evolutionary biology (Balkenhol *et al.* 2009b; Jaquiéry *et al.* 2011). Hundreds of landscape genetics studies have now been published, but a recent meta-analysis detected few general trends in genetic responses to landscape characteristics (Storfer *et al.* 2010). These findings indicate the importance of studying many taxonomic groups across a range of landscape heterogeneity.

Landscape genetic studies on mammals have tended to focus on large-bodied and/or wide-ranging species (Broquet *et al.* 2006; Epps *et al.* 2007; McRae & Beier 2007; Perez-Espona *et al.* 2008; Pease *et al.* 2009; Hapeman *et al.* 2011). The spatial scale, time since landscape features have changed, and life history traits of the study taxa all influence landscape genetic results (Anderson *et al.* 2010). The importance of different landscape elements for the same species may also vary between study sites (Short Bull *et al.* 2011). For these reasons, previous results are unlikely to predict spatial genetic structure in small mammals with limited dispersal abilities. Landscape data that are sufficiently fine-grained to reflect the scale of migration distances, and thorough genetic sampling from multiple populations in that landscape, will likely be necessary for smaller taxa (Anderson *et al.* 2010).

Simulation studies predict that landscape genetic approaches will be most successful when applied to simple landscapes comprised of elements that differ strongly in their ability to impede migration (Jaquiéry *et al.* 2011). Urbanization produces landscapes with these characteristics, often resulting in homogenization of biodiversity as a small number of 'urban adapters' thrive at the expense of urban-sensitive taxa (McKinney 2006). Urban habitat patches are typically small, fragmented and surrounded by a matrix of roads and buildings that begins immediately outside the discrete edges of the patch. This matrix is relatively impermeable to many small vertebrates, and multiple studies have now reported substantial genetic differentiation between isolated urban populations of native species (Bjorklund *et al.* 2010; Delaney *et al.* 2010; Noël & Lapointe 2010). Human commensals such as the Norway rat (*Rattus norvegicus*) are exceptional in exhibiting moderate gene flow through urban landscapes (Gardner-Santana *et al.* 2009). However, city parks and private gardens may form networks of green space that promote limited connectivity for some native taxa (Goddard *et al.* 2010). Given near-binary habitat distributions and potential linear corridors comprised of artificial or semi-natural landscape elements (e.g. roadway medians, Pećarević *et al.* 2010), landscape genetic relationships are likely to be found in urban environments. However, no study to date has examined spatial associations between landcover and genetic connectivity in the urban core.

In this study, I examine statistical associations between urban tree canopy cover and multiple measures of genetic connectivity between white-footed mice (*Peromyscus leucopus*) sampled from 15 populations in New York City (NYC), USA. Previous analyses showed that nearly all of these sites contained genetically distinct subpopulations with moderate to high genetic variation, although some admixture was detected between proximal areas (Munshi-South & Kharchenko 2010). White-footed mice are found in nearly every forested area in NYC that has been surveyed, but are replaced by house mice (*Mus musculus*) and Norway rats in the urban matrix (J. Munshi-South, unpublished data). Tree canopy cover was thus chosen as the primary landscape variable for this study because of its potential role in determining the distribution of *P. leucopus* in the urban core. Population densities of white-footed mice are typically much higher in fragmented vs. undisturbed environments (Nupp & Swihart 1996; Krohne & Hoch 1999; Rytwinski & Fahrig 2007), and elevated intraspecific competition in these fragments contributes to higher emigration rates (Anderson & Meikle 2010).

Given the apparent ecological success and genetic variability of *P. leucopus* in urban forest fragments (Munshi-South & Kharchenko 2010), it is likely that this species has the ability for limited migration through the urban core. Urban fragments in NYC are highly isolated, but the ecological thresholds (if they exist) beyond which connectivity breaks down are currently unknown. Opportunistic trapping records at the edges

of forest fragments in NYC indicate that white-footed mice occupy or move through even the thinnest, marginal green spaces (i.e. unmowed fencerows, cemetery edges and roadside vegetation). Breeding populations have also been recorded in long, linear forested parklands that are only a few tens of metres wide (e.g. Highbridge Park in NW Manhattan, J. Munshi-South, unpublished data), suggesting that gene flow between major park populations can occur across generations rather than through direct dispersal. By comparing relative migration rates between forest fragments separated by varying amounts and configurations of 'green' and 'grey' infrastructure, landscape genetics approaches can identify the most likely features of the urban core that promote migration. *P. leucopus* are nearly ubiquitous in forest fragments in NYC, but less abundant sympatric species such as the meadow vole (*Microtus pennsylvanicus*) or short-tailed shrew (*Blarina brevicauda*) are likely to migrate along the same pathways (or may if the green infrastructure was improved). White-footed mice are also prey for a number of species in the northeastern United States. Understanding the dynamics of migration in the urban landscape can help inform management of urban predators, particularly raptors such as the Eastern screech owl (*Megascops asio*), that have been re-introduced and are actively monitored in NYC (Nagy *et al.* in press).

Here, I use a data set of 18 microsatellite genotypes to estimate both recent and longer-term migration rates between white-footed mouse populations in NYC. Then, I examine the correlation between these population genetic measures and different spatial models of population connectivity based on tree canopy cover in NYC. Multiple connectivity models were generated by assigning low resistance to sequentially lower percentages of canopy cover to examine whether additional low-resistance habitat increased the correlation between canopy cover and migration.

Peromyscus leucopus individuals may disperse several kilometres from capture sites (Maier 2002), but most studies have not recorded average dispersal distances greater than 500 m (Stickel 1968). Thus, IBD alone may be sufficient to explain how the urban landscape structures white-footed mouse populations in NYC: migration rates should decrease with Euclidean distance between populations. If the composition of the urban landscape plays a role in genetic structuring, then white-footed mice should migrate along pathways of preferred, or at least sublethal, landscape elements. The least-cost path, or 'isolation-by-effective-distance' (IED), approach calculates the single best path that will minimize accumulated costs as an animal moves through a hypothetical landscape resistance surface (Sawyer *et al.* 2011). Although more biologically realistic than IBD, IED approaches still suffer from the simplistic assumption of a single path through the landscape (Rayfield *et al.* 2010). A recently developed implementation of circuit theory, known as isolation by resistance (IBR), models adjacent landscape cells as series of electrical resistors to calculate an overall resistance distance between populations (McRae 2006). The resistance distance is theoretically related to random walk times through all possible landscape paths and may outperform IBD and IED in predicting gene flow and genetic differentiation (McRae & Beier 2007).

In this study, I test the prediction that migration rates between urban white-footed mouse populations are associated with landscape connectivity models based on the amount and configuration of tree canopy cover in NYC. I use the estimated migration rates and connectivity maps to identify the most likely corridors of movement through the urban core for this species. Secondarily, I examine whether IBR and IED models based on canopy cover will outperform IBD, and whether IBR will outperform IED, at explaining genetic differentiation and gene flow among urban white-footed mouse populations. IBR and IED models may produce spurious correlations if their effects are confounded with each other or Euclidean distance, so I used partial Mantel tests to identify the best models while controlling for alternative scenarios (Cushman & Landguth 2010). Finally, I test the hypothesis that recent migration rates between urban populations using BayesAss+ will be correlated with higher percentages of canopy cover than longer-term migration estimates from F_{ST}-based *Nm* or Migrate-*n*. Given that urbanization has likely reduced connectivity between populations in NYC over time, migration may have been partly shaped by pathways that are absent or degraded in the contemporary landscape.

Methods

Study sites, sampling and population genetic data

I conducted trapping surveys at 15 sites in NYC (Fig. 1) from June 2008 to October 2009 and collected tail snips for genetic analysis from all unique individuals (see Table 1 for sample sizes). All 294 sampled individuals were then genotyped at 18 unlinked microsatellite loci. These genotypes were previously analysed to examine genetic differentiation between urban populations, and Munshi-South & Kharchenko (2010) provide full details of sampling and genotyping. The genotypes and spatial coordinates for all study sites are available on the Dryad digital repository (doi: 10.5061/dryad.7gh65757).

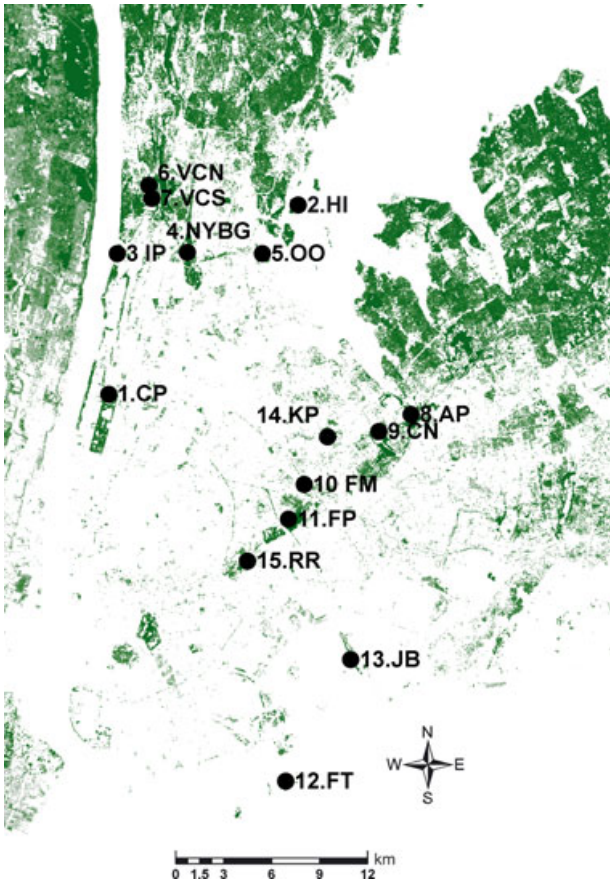

Fig. 1 Fifteen white-footed mouse locations sampled in New York City. The Bronx/Manhattan cluster is comprised of sites 1–7, and the Queens cluster of sites 8–15. 1. CP = Central Park, 2. HI = Hunter Island, 3. IP = Inwood Hill Park, 4. NYBG = New York Botanical Garden, 5. OO = Southwestern Pelham Bay Park, 6. VCN = Van Cortlandt Park north of Henry Hudson Parkway, 7. VCS = Van Cortlandt Park south of Henry Hudson Parkway, 8. AP = Alley Pond Park, 9. CN = Cunningham Park, 10. FM = Flushing Meadows—Willow Lake, 11. FP = Forest Park, 12. FT = Fort Tilden, 13. JB = Jamaica Bay, 14. KP = Kissena Park, 15. RR = Ridgewood Reservoir—Highland Park.

For downstream landscape genetic analyses, study sites were analysed as one of two geographically separated clusters: (i) Bronx & Manhattan (Sites 1–7; Fig. 1), (ii) Queens (Sites 8–15; Fig. 1). Previous analysis confirmed all 15 sites as unique evolutionary clusters (Munshi-South & Kharchenko 2010). However, Queens is separated from Manhattan and Bronx by the formidable barriers of the East River and Long Island Sound, and thus recent gene flow has likely been negligible between the two population clusters. In contrast, Manhattan is separated from the Bronx at its northern tip by the narrow Spuyten Duyvil Creek, and forested parklands exist on both shores. This tidal channel was meandering, narrow and often very shallow during low tides before being dredged and straightened as a shipping canal from 1888 to 1895 (Horenstein 2007); today, the shipping channel is approximately 120 m wide. Although few data exist, *Peromyscus* spp. have been observed swimming up to 233 m (reviewed in Schoener & Schoener 1984). To reach Queens from either the Bronx or Manhattan, however, would require longer aquatic movements through strong currents. Additionally, the Queens coastline across from the two other landmasses is largely nonvegetated industrial or residential space rather than parklands (Fig. 1). The assumption that Bronx and Manhattan populations are much more likely to have historical connectivity than either with Queens is also supported by previous results. Although differences between populations exceeded differences between landmasses in the earlier study, an evolutionary cluster analysis with $k = 6$ received the second highest level of support after $k = 16$. For $k = 6$, the Van Cortlandt (VCN and VCS in Fig. 1) populations in the Bronx and the Inwood (IP) population at the tip of Manhattan were part of the same evolutionary cluster, indicating the greater likelihood of connectivity between these two landmasses (Fig. S1 in Supporting information, Munshi-South & Kharchenko 2010).

Estimates of gene flow

To estimate population differentiation and migration, I calculated pairwise linearized F_{ST} as (F_{ST}/[1−F_{ST}], Table S1, Supporting information) and *Nm* as ([(1/F_{ST})−1]/4), between all possible pairs in the two population clusters using GenAlex 6.4 (Peakall & Smouse 2006). Statistical significance was assessed by *P*-values calculated using 10 000 random permutations of the data and a Bonferroni correction. This statistic is a symmetric average of migration in both directions between two populations and thus has no information on directionality. Two other estimators of migration below were calculated in each direction between each pair of populations, and the migration estimates in each direction were analysed separately to preserve the directionality of migration. *Nm* from F_{ST} was included in this study for comparative purposes with the many past studies that have used approaches based on *F*-statistics.

To estimate recent migration rates, I used the Bayesian estimator implemented in BayesAss+ 1.3 (Wilson & Rannala 2003). Migration rate estimates in BayesAss+ are based on the proportion of individuals in each population sample that are assigned to other populations with high probability. The program is successful at detecting migration based on individual migrant

Table 1 Euclidean geographic distances (kilometres; above diagonal) and *Nm* calculated from F_{ST} ($Nm = [(1/F_{ST}) - 1]/4$; below diagonal) estimated between each pair of populations in the Bronx & Manhattan (top) and Queens (bottom)

	1. CP	2. HI	3. IP	4. NYBG	5. OO	6. VCN	7. VCS	
1. CP (*N* = 15)	–	16.78	8.85	10.18	13.05	13.36	12.60	
2. HI (27)	2.45	–	11.72	7.53	3.78	9.41	9.16	
3. IP (20)	3.22	3.27	–	4.40	9.08	4.73	4.09	
4. NYBG (33)	2.27	2.45	3.78	–	4.68	4.86	4.07	
5. OO (14)	2.01	2.51	2.92	2.94	–	8.29	7.74	
6. VCN (10)	2.59	2.23	3.57	3.24	3.03	–	0.83	
7. VCS (14)	3.00	3.23	4.01	3.47	3.69	6.24	–	
	8. AP	9. CN	10. FM	11. FP	12. FT	13. JB	14. KP	15. RR
8. AP (*N* = 9)	–	2.28	7.98	10.07	24.28	15.80	5.39	13.72
9. CN (25)	5.92	–	5.71	7.86	22.67	14.39	3.22	11.52
10. FM (30)	3.32	5.32	–	2.39	18.66	11.38	3.30	5.96
11. FP (11)	4.72	7.59	4.95	–	16.45	9.64	5.69	3.66
12. FT (18)	2.41	2.78	1.72	2.16	–	8.65	21.74	14.03
13. JB (11)	2.87	3.48	2.32	3.24	1.86	–	14.02	8.94
14. KP (24)	3.19	2.87	2.35	3.48	2.16	2.22	–	9.23
15. RR (33)	3.71	4.65	3.33	5.65	1.97	2.61	3.05	–

Sample sizes (*N*) appear next to each population in the first column.
1. CP, Central Park; 2. HI, Hunter Island; 3. IP, Inwood Hill Park; 4. NYBG, New York Botanical Garden; 5. OO, Southwestern Pelham Bay Park; 6. VCN, Van Cortlandt Park north of Henry Hudson Parkway; 7. VCS, Van Cortlandt Park south of Henry. Hudson Parkway; 8. AP, Alley Pond Park; 9. CN, Cunningham Park; 10. FM, Flushing Meadows—Willow Lake; 11. FP, Forest Park; 12. FT, Fort Tilden; 13. JB, Jamaica Bay; 14. KP, Kissena Park; 15. RR, Ridgewood Reservoir.

ancestries within a few generations and relaxes some equilibrium assumptions (e.g. Hardy–Weinberg but not linkage equilibrium). A recent simulation study (Faubet *et al*. 2007) indicated that BayesAss+ produces accurate migration estimates when genetic differentiation is not too low ($F_{ST} \geq 0.05$), an assumption that holds for population pairs in this study (Table S1, Supporting information). Separate analyses were run for the Bronx/Manhattan and Queens population clusters using a burn-in of 1 000 000 steps of 5 000 000 total iterations, and a sampling frequency of 2000 iterations. The default delta value of 0.15 was used for allele frequency, migration rate and inbreeding. Here, I report the migration rates calculated between each population pair in each direction (Table 2), and the corresponding 95% confidence intervals (Table S2, Supporting information). BayesAss+ also reports the 95% confidence intervals expected for uninformative data, and I used these data to assess the reliability of the estimated migration rates. For seven populations, uninformative data will produce 95% confidence intervals for migration rates of 0–0.144, and 95% confidence intervals for proportion of residents of 0.675–0.992. For eight populations, uninformative data will produce 95% CIs for migration rates of 0–0.134, and the same 95% CIs for residents as for seven populations.

I also used the Bayesian coalescent approach implemented in Migrate-*n* to estimate migration rates between populations (Beerli 2006). This method produces estimates of θ ($4N_e\mu$, where μ = mutation rate) and M (m/μ, where m = migration rate) for microsatellite data from n populations. As with Nm from F_{ST}, the migration rates are an average over many generations back in time and assume that the system is in migration–drift equilibrium. To estimate migration, I ran five replicates for each population cluster in Migrate-*n* using a Brownian motion mutation model with constant mutation rates and starting parameters based on F_{ST} calculations. An exponential prior distribution (range = 0–100, mean = 50) was used to estimate θ, and a uniform prior distribution (range = 0–100, mean = 50, delta = 10) was used for M. The priors were chosen based on the performance of multiple trial runs with different prior values. Each of the five replicate runs visited a total of 5 000 000 parameter values including a 500 000 burn-in period, and sampled the parameter value every 100 iterations. I used the median value of M from each run's posterior distribution to calculate an overall mean M for each population pair in each direction. Here, I report these mean migration rates (Table 3) and the 0.025 and 0.975 posterior distribution values (Table S3, Supporting information) as 95% confidence interval

Table 2 Recent migration rates estimated between each pair of populations in the Bronx & Manhattan (top) and Queens (bottom) using BayesAss+ 1.3

	1. CP	2. HI	3. IP	4. NYBG	5. OO	6. VCN	7. VCS	
1. CP	**0.98**	0.002	0.006	0.002	0.004	0.015	0.006	
2. HI	0.003	**0.988**	0.006	0.002	0.006	0.014	0.01	
3. IP	0.003	0.002	**0.974**	0.002	0.004	0.124	0.02	
4. NYBG	0.003	0.002	0.003	**0.99**	0.004	0.015	0.007	
5. OO	0.003	0.002	0.004	0.001	**0.975**	0.015	0.006	
6. VCN	0.003	0.002	0.003	0.002	0.004	**0.695**	0.006	
7. VCS	0.003	0.002	0.004	0.002	0.004	0.122	**0.944**	
	8. AP	9. CN	10. FM	11. FP	12. FT	13. JB	14. KP	15. RR
8. AP	**0.696**	0.002	0.001	0.011	0.002	0.011	0.002	0.004
9. CN	0.226	**0.985**	0.002	0.077	0.002	0.027	0.004	0.004
10. FM	0.013	0.003	**0.99**	0.012	0.002	0.011	0.005	0.004
11. FP	0.014	0.002	0.002	**0.693**	0.002	0.011	0.003	0.004
12. FT	0.013	0.002	0.001	0.011	**0.984**	0.226	0.003	0.004
13. JB	0.012	0.002	0.001	0.01	0.002	**0.693**	0.003	0.004
14. KP	0.013	0.002	0.001	0.173	0.002	0.011	**0.978**	0.301
15. RR	0.013	0.002	0.001	0.012	0.002	0.01	0.003	**0.676**

Values above the diagonal (top matrix) are migration rates from the populations in the horizontal row into the populations in the vertical column, and values below the diagonal (bottom matrix) are migration rates from the populations in the vertical column into the populations in the horizontal row. The diagonal values in bold are the percentages of resident individuals in each population per generation.

1. CP, Central Park; 2. HI, Hunter Island; 3. IP, Inwood Hill Park; 4. NYBG, New York Botanical Garden; 5. OO, Southwestern Pelham Bay Park; 6. VCN, Van Cortlandt Park north of Henry Hudson Parkway; 7. VCS, Van Cortlandt Park south of Henry. Hudson Parkway; 8. AP, Alley Pond Park; 9. CN, Cunningham Park; 10. FM, Flushing Meadows—Willow Lake; 11. FP, Forest Park; 12. FT, Fort Tilden; 13. JB, Jamaica Bay; 14. KP, Kissena Park; 15. RR, Ridgewood Reservoir.

estimates (Beerli & Felsenstein 2001) of the median for each of the five runs.

Calculation of Euclidean, effective and resistance distances

Pairwise Euclidean distances between populations were calculated for each population cluster using the Landscape Genetics ArcToolbox (Etherington 2011) in ArcGis 9.3 (ESRI). Calculation of effective and resistance distances required spatial data sets on landcover in NYC and hypotheses about the relative permeability of landscape elements to migration between white-footed mouse populations. I used percentage tree canopy cover as the primary variable for examining influences of the landscape on genetic structure because of its likely role in influencing the distribution of white-footed mice and other forest species in NYC. Raster images of per cent tree canopy at 30-m resolution (Fig. 1) were downloaded from the 2001 National Land Cover Database (Homer *et al.* 2004), and the continuous percentages were lumped into categorical bins of 10% canopy cover using ArcGIS (e.g. 0–9%, 10–19%; Table S4, Supporting information). The spatial extent of the data used for this study included the entire land area of NYC (excluding Staten Island), Westchester Co., NY, north of the Bronx, and Nassau Co., NY, east of Queens. Areas west and south of NYC were excluded because of the Hudson River and oceanic barriers to migration in these directions.

To examine associations between gene flow and the spatial configuration of low-resistance habitat, I recoded each 30-m cell of the canopy cover data set with resistance values of either 1 = no or low resistance, or 10 000 = high, quasi-barrier resistance. Nine different resistance grids were created to examine the effect of lowering the resistance for sequentially lower levels of tree canopy cover (Table S4, Supporting information). In other words, in the first scenario, only 30-m cells with 90% or greater canopy cover were coded as low resistance, but in the ninth scenario, all cells with 10% or greater canopy cover were coded as low resistance. The alternative hypothesis that migration will decrease gradually with less canopy cover could not be assessed using these resistance scenarios. However, given the complete absence of white-footed mice outside vegetated areas in NYC, I predicted that gene-flow measures would correlate most strongly with scenarios of abrupt

Table 3 Unidirectional migration rates, M (m/μ), estimated between each pair of populations in the Bronx & Manhattan (top) and Queens (bottom) using Migrate-*n* 3.2.1

	1. CP	2. HI	3. IP	4. NYBG	5. OO	6. VCN	7. VCS	
1. CP	–	2.79	3.97	2.25	5.90	7.90	6.20	
2. HI	5.49	–	5.46	2.95	6.53	10.05	7.34	
3. IP	6.97	3.07	–	2.31	8.14	9.69	10.59	
4. NYBG	7.76	4.37	4.81	–	7.75	8.57	6.87	
5. OO	4.57	2.77	4.03	2.26	–	8.38	7.59	
6. VCN	6.07	2.80	4.53	2.27	5.31	–	5.12	
7. VCS	4.59	3.39	3.66	2.33	5.62	8.70	–	
	8. AP	9. CN	10. FM	11. FP	12. FT	13. JB	14. KP	15. RR
8. AP	–	2.86	2.47	4.98	3.32	7.14	2.97	2.43
9. CN	10.41	–	3.11	9.57	5.66	9.53	4.43	2.70
10. FM	7.40	4.06	–	5.83	4.86	5.82	3.82	2.83
11. FP	9.01	3.18	2.46	–	4.41	4.74	2.69	2.21
12. FT	7.70	3.15	2.74	5.18	–	8.14	3.11	2.40
13. JB	6.77	3.22	2.30	6.57	4.71	–	3.02	2.30
14. KP	7.33	2.95	2.62	7.03	5.73	6.88	–	2.65
15. RR	7.03	4.22	3.14	8.42	4.87	9.87	3.97	–

Values presented are the average median M calculated from five independent runs of Migrate-*n*. Values above the diagonal (top matrix) are migration rates from the populations in the horizontal row into the populations in the vertical column, and values below the diagonal (bottom matrix) are migration rates from the populations in the vertical column into the populations in the horizontal row.

1. CP, Central Park; 2. HI, Hunter Island; 3. IP, Inwood Hill Park; 4. NYBG, New York Botanical Garden; 5. OO, Southwestern Pelham Bay Park; 6. VCN, Van Cortlandt Park north of Henry Hudson Parkway; 7. VCS, Van Cortlandt Park south of Henry. Hudson Parkway; 8. AP, Alley Pond Park; 9. CN, Cunningham Park; 10. FM, Flushing Meadows—Willow Lake; 11. FP, Forest Park; 12. FT, Fort Tilden; 13. JB, Jamaica Bay; 14. KP, Kissena Park; 15. RR, Ridgewood Reservoir.

disruption of migration after canopy cover reaches a critical low level. These nine resistance grids are available on Dryad (doi: 10.5061/dryad.7gh65757).

Effective distances between populations were calculated under all nine canopy resistance scenarios using the 'least-cost paths' tool in the Landscape Genetics ArcToolbox. This analysis outputs a pairwise matrix of the length of the single best path between populations that minimizes the cumulative resistance cost (e.g. passes through the fewest cells with resistance = 10 000), as well as a polyline file of the path itself. Pairwise resistance distances between populations for all nine canopy scenarios were calculated using Circuitscape 3.5 (Shah & McRae 2008). In these analyses, populations were treated as focal points consisting of a single cell, and adjacent cells were connected to eight neighbours by average resistances. This analysis proceeds by designating one focal population as an electrical source and the receiving population as an electrical ground. Each landscape cell is assumed to be connected to adjacent cells by electrical resistors, each of which impedes current flow to different degrees depending on the resistance values set by the researcher. Circuitscape then calculates a pairwise matrix of the effective resistance distances between populations and can also generate a cumulative 'current map' portraying areas where resistance to gene flow is relatively low or high. The latter analysis is computationally intensive, so current maps were generated *post hoc* only for resistance distances that were highly correlated with gene-flow estimates. These analyses are biologically relevant to dispersal and gene flow because resistance distances are highly correlated with random walk times through landscapes.

Testing IBD, IED and IBR models of landscape influence on gene flow

Pairwise measures of Euclidean, effective and resistance distances were ln-transformed to improve linearity for tests of statistical association with migration estimates. To test IBD models, I used the 'ecodist' package (Goslee & Urban 2007) in R (R Development Core Team 2008) to run simple Mantel tests of the association between pairwise matrices of the three gene-flow estimates and ln Euclidean distance for the two population clusters. Statistical significance of all Mantel tests was assessed using 10 000 randomizations of the matrix values, and 95% confidence intervals for the Mantel correlation coefficient r were estimated using 10 000 bootstrap

iterations that resampled 90% of the data. Statistical associations between all nine IED models (ln effective distance) and migration estimated from *Nm*, BayesAss+ and Migrate-*n* were also calculated using simple Mantel tests in 'ecodist' for the two population clusters. These analyses were repeated for all nine IBR models. To preserve the directional information in the BayesAss+ and Migrate-*n* migration rates, I ran separate Mantel tests on both the top and bottom halves of the pairwise matrices (Tables 2–3).

If canopy cover with low resistance to migration occurs linearly in the NYC landscape, then IED and IBR models may be highly correlated with gene flow owing to the effects of IBD (Cushman & Landguth 2010). To control for the confounding influence of IBD, I calculated partial Mantel tests in a stepwise modelling framework in 'ecodist'. Partial Mantel tests examined the association between one pairwise matrix of effective distances and one pairwise matrix of gene flow while controlling for the effects of a pairwise matrix of Euclidean distances between populations. For IBR calculations, I calculated 'flat' resistance distances on a uniform landscape of no resistance in Circuitscape that was used in place of the Euclidean distance matrix. Euclidean distances and these flat resistance distances were highly correlated (Mantel $r = 0.99$, $P < 0.0001$). As above, partial Mantel correlations and confidence intervals were estimated for all possible combinations of the nine IED/IBR models and the three measures of gene flow to determine which IBR and IED models explained genetic structure better than IBD. In cases where both IED and IBR models significantly explained gene flow after controlling for IBD, I ran an additional partial Mantel test to choose between the IED and IBR models.

Results

Estimates of population differentiation and gene flow

All linearized pairwise F_{ST} values were statistically significant ($P < 0.0001$; Table S1, Supporting information) between white-footed mouse populations in NYC. Linearized F_{ST} ranged from 0.04 to 0.125 among population pairs in Bronx and Manhattan, and from 0.033 to 0.145 among Queens pairs (Table S1, Supporting information). The *Nm* values calculated from F_{ST} were all greater than zero, ranging from 1.7 to 7.6 (Table 1). Recent migration rates estimated in BayesAss+ were very low for most population pairs (Table 2), and these low values typically had 95% confidence intervals with a lower bound near zero (Table S2, Supporting information). Nearly all of the estimated 95% confidence intervals were much narrower than those expected for uninformative data (see Methods above), indicating that the estimates reported here were produced from informative data. The median values of migration rates *M* estimated in Migrate-*n* were uniformly greater than zero, ranging from 2.31 to 10.59 in Bronx and Manhattan and from 2.21 to 10.41 in Queens (Table 3). However, a moderate number of these values also had 95% confidence intervals with lower bounds at or near zero (Table S3, Supporting information).

Simple Mantel tests of IBD, IED and IBR and gene-flow estimates

IBD significantly explained migration estimated from *Nm* and BayesAss+, but not Migrate-*n*, in both Bronx and Manhattan and Queens (Table 4). However, the 95% confidence intervals for migration from BayesAss+ overlapped zero, indicating that the significant result may have been driven by one or a few values. IBD explained *Nm* patterns in Bronx and Manhattan better than among Queens populations.

All nine IED models were significantly associated with *Nm* and the bottom matrix of BayesAss+ estimates, but not the top matrix from BayesAss+ or either matrix from Migrate-*n*, in both population clusters (Table S5, Supporting information). All nine IBR models were significantly associated with *Nm* and the bottom matrix from BayesAss+ in both population clusters. IBR models were not significantly correlated with Migrate-*n*

Table 4 Results of simple Mantel tests for isolation by distance (IBD) between ln-transformed Euclidean distances and three pairwise measures of genetic connectivity

Genetic statistic	Bronx & Manhattan	Queens
Nm from F_{ST}	$r =$ **−0.806** (−0.944 to −0.371)**	**−0.499** (−0.685 to −0.277)*
Recent migration (bottom matrix—Table 2)	**−0.723** (−0.875–0.484)*	**−0.396** (−0.605–0.027)*
Recent migration (top matrix—Table 2)	−0.14 (−0.434–0.091)	0.005 (−0.112–0.167)
Historical migration (bottom matrix—Table 3)	0.026 (−0.42–0.61)	0.042 (−0.236–0.291)
Historical migration (top matrix—Table 3)	−0.12 (−0.373–0.15)	0.153 (0.007–0.31)

*$P \leq 0.05$; **$P \leq 0.001$. Values in bold are statistically significant.
95% confidence intervals estimated using 10 000 bootstrap replicates in the 'ecodist' package in R appear in parentheses next to Mantel correlation coefficients.

estimates in Bronx and Manhattan, but eight of nine IBR models were significantly associated with the bottom matrix from Migrate-*n* in Queens (Table S5, Supporting information).

Identification of best landscape genetic models using partial Mantel tests

After controlling for Euclidean distance in partial Mantel tests, three IED models and seven IBR models for Bronx and Manhattan were significantly correlated with *Nm* (Fig. 2a). One IED model and three IBR models were significantly associated with *Nm* in Queens (Fig. 3a). Seven IBR models were correlated (partial Mantel $r \leq -0.9$) with the bottom matrix from BayesAss+ in Bronx & Manhattan after controlling for IBD and exhibited very narrow 95% confidence intervals (Fig. 2b). However, no models were correlated with the top matrix from BayesAss+ in either population cluster (Figs 2c and 3c). All nine IBR and three IED models were correlated with the bottom matrix from BayesAss+ in Queens independent of IBD (Fig. 3b). Seven IBR models in Bronx & Manhattan (Fig. 2d) and eight IBR models in Queens (Fig. 3d) were significantly associated with the bottom matrix from Migrate-*n* after controlling for IBD. One IED model in Bronx and Manhattan (Fig. 2e), and no models in Queens (Fig. 3e), was significantly associated with the top matrix from Migrate-*n*. None of the 95% confidence intervals calculated from bootstrapping the statistically significant partial Mantel correlation coefficients overlapped zero, indicating that the significant tests were not driven by high-leverage, outlier values.

In Bronx and Manhattan, an IED model that assigned high resistance to areas with <30% canopy cover best explained *Nm* (partial Mantel $r = 0.79$, $P < 0.001$; Fig. 4a), whereas an IBR model of high resistance for <70% canopy was most highly correlated with BayesAss+ ($r = -0.94$, $P < 0.001$) and Migrate-*n* ($r = -0.54$, $P < 0.01$; Fig. 4b) estimates. Results from IBR models that assigned low resistance to 70% or less canopy cover (scenarios 3–9 in Table S4, Supporting information) produced nearly indistinguishable results for the bottom matrices from BayesAss+ and Migrate-*n* (Fig. 2b,d).

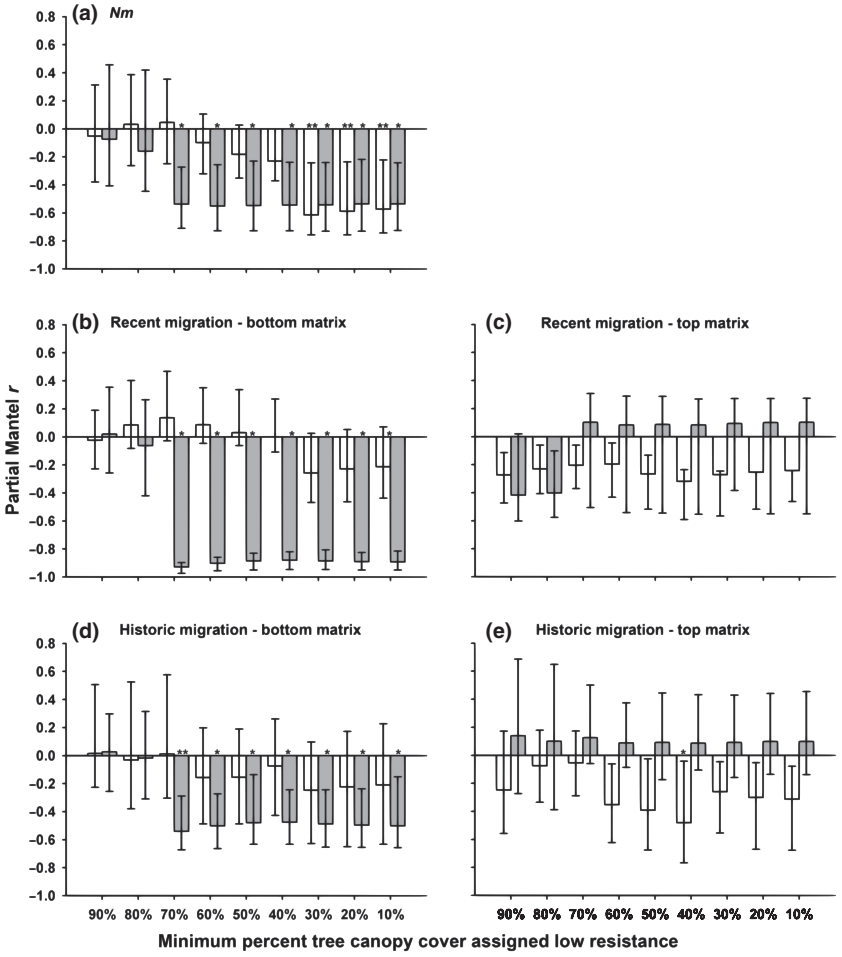

Fig. 2 Partial Mantel correlation coefficients calculated while controlling for isolation by distance among Bronx and Manhattan populations using (a) *Nm* calculated from F_{ST} in Table 1, (b) the bottom matrix of recent migration rates from BayesAss+ in Table 2, (c) the top matrix of recent migration rates from BayesAss+ in Table 2, (d) the bottom matrix of migration rates from Migrate-*n* in Table 3 and (e) the top matrix of migration rates from Migrate-*n* in Table 3. White bars represent isolation-by-effective-distance models, and grey bars represent isolation-by-resistance models. Error bars are the 95% confidence intervals from 10 000 bootstrap replicates of the partial Mantel correlation coefficients. $^{*}P < 0.05$, $^{**}P < 0.01$.

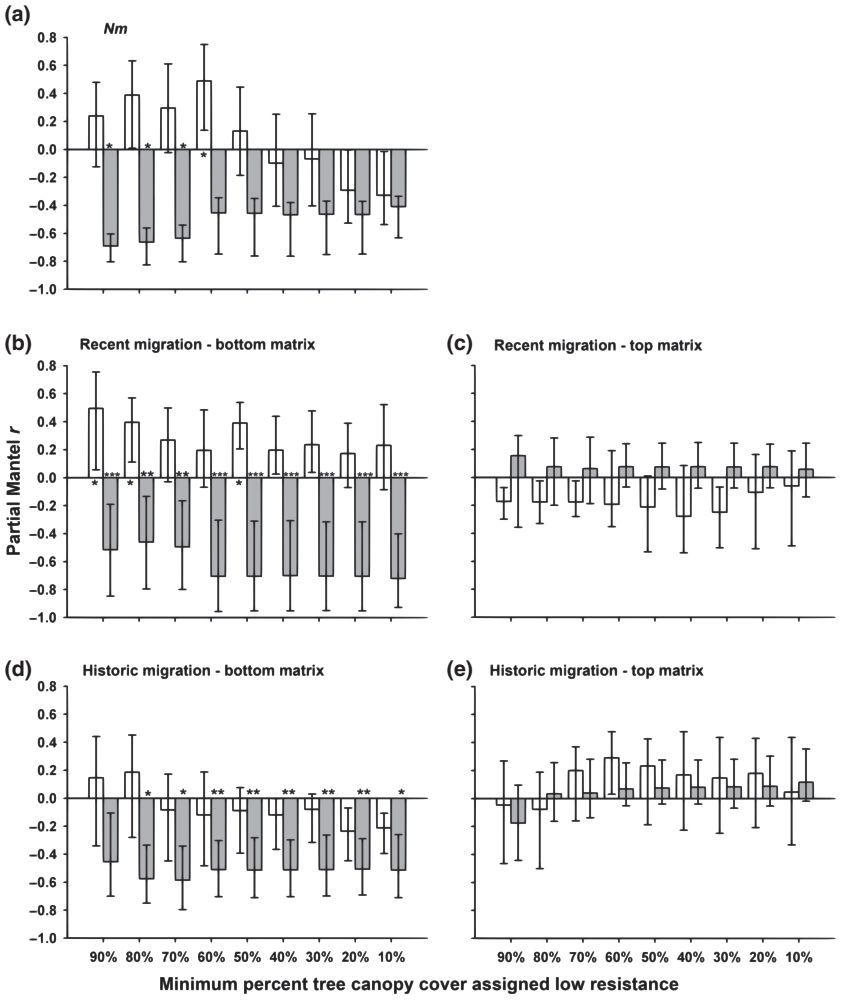

Fig. 3 Partial Mantel correlation coefficients calculated while controlling for isolation by distance among Queens populations using (a) *Nm* calculated from F_{ST} in Table 1, (b) the bottom matrix of recent migration rates from BayesAss+ in Table 2, (c) the top matrix of recent migration rates from BayesAss+ in Table 2, (d) the bottom matrix of migration rates from Migrate-*n* in Table 3, and (e) the top matrix of migration rates from Migrate-*n* in Table 3. White bars represent isolation-by-effective-distance models, and grey bars represent isolation-by-resistance models. Error bars are the 95% confidence intervals from 10 000 bootstrap replicates of the partial Mantel correlation coefficients. $^{*}P < 0.05$, $^{**}P < 0.01$, $^{***}P < 0.001$.

In Queens, the bottom matrix from BayesAss+ was correlated with both IED and IBR models: the former with high resistance for <90% forest cover ($r = 0.55$, $P < 0.01$; Fig. 5a), and the latter with high resistance for <10% forest cover ($r = -0.72$, $P < 0.0001$; Fig. 5d). *Nm* was most strongly associated with an IBR model of high resistance for <90% canopy cover in Queens ($r = 0.63$, $P < 0.05$; Fig. 5b). An IBR model of high resistance for <70% canopy cover was most strongly associated with the bottom matrix from Migrate-*n* in Queens ($r = -0.59$, $P < 0.05$; Fig. 5c). However, results from IBR models that assigned low resistance to 80% or less canopy cover (scenarios 2–9 in Table S4, Supporting information) produced similar results for the bottom matrices from BayesAss+ and Migrate-*n* (Fig. 3b,d). As IBR models assigned low resistance to lower and lower percentages of canopy cover, the overall area of connectivity along Queens' central corridor of parklands roughly stayed the same (Fig. 5b–d). However, many more discrete paths of high connectivity were estimated for the lowest-resistance models (Fig. 5d).

IED and IBR models were both successful at explaining patterns of *Nm* in the two population clusters after controlling for IBD (Figs 2a and 3a). In the Bronx and Manhattan, the best IBR model (Scenario 4) was still highly correlated with *Nm* (partial Mantel $r = -0.509$, $P < 0.05$; 95% CI = −0.652 to −0.366) after controlling for the best IED model (Scenario 7). However, the best IED model explained nearly the same amount of variation in *Nm* after controlling for the best IBR model ($r = -0.546$, $P < 0.05$, 95% CI = −0.639 to −0.445). In Queens, the best IBR model (Scenario 1) was still highly correlated with *Nm* (partial Mantel $r = -0.718$, $P < 0.05$; 95% CI = −0.822 to −0.638) after controlling for the best IED model (Scenario 4). However, the best IED model explained almost no variation in BayesAss+ estimates after controlling for the best IBR model ($r = -0.076$, $P = 0.39$, 95% CI = −0.501–0.32), indicating that IBR was the superior model.

IED and IBR models were both successful at explaining the bottom matrix from BayesAss+ in Queens after controlling for IBD (Fig. 3b), but only IBR models were

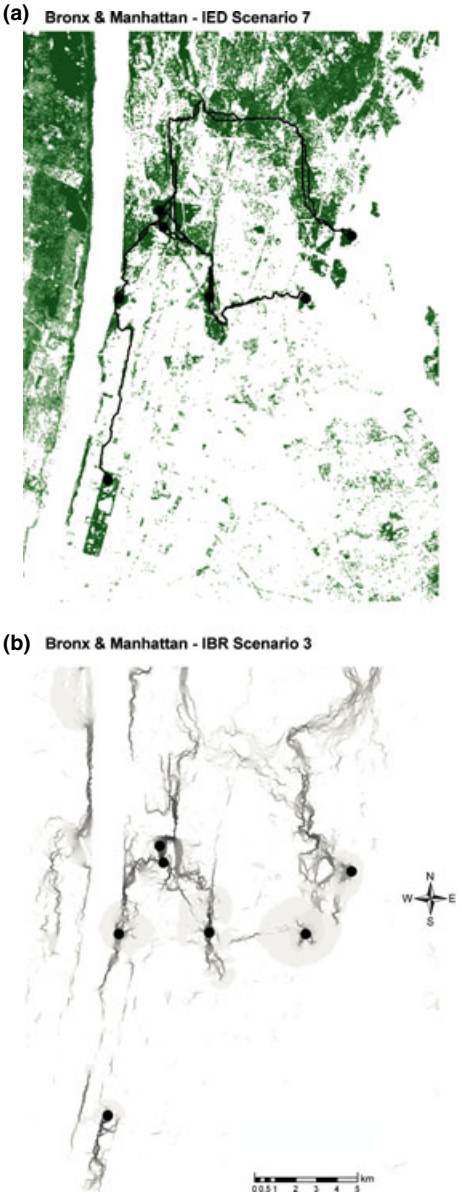

Fig. 4 Landscape models with highest partial Mantel *r* correlation coefficients for Bronx and Manhattan populations of white-footed mice: (a) isolation-by-effective-distance model (IED; based on low resistance for 30% or more canopy cover) that was most strongly correlated with *Nm* from F_{ST} and (b) isolation-by-resistance model (IBR; based on low resistance for 70% or more canopy cover) that was most strongly correlated with both recent and longer-term migration rates.

successful in the Bronx and Manhattan (Fig. 2b). The best IBR model (Scenario 9) in Queens was still highly correlated with BayesAss+ estimates (partial Mantel $r = -0.73$, $P < 0.0001$; 95% CI = −0.94 to −0.375) after controlling for the best IED model (Scenario 1). However, the best IED model explained almost no variation in BayesAss+ estimates after controlling for the best IBR model ($r = 0.07$, $P = 0.39$, 95% CI = −0.036–0.345), indicating that IBR was the superior model.

Urban landscape features identified as low-resistance corridors for migration

The best IBR and IED models both estimated that migration occurs through cemeteries or along vegetated medians of automobile parkways in the central Bronx, and through corridors of forest cover in Westchester Co. north of the Bronx (Fig. 4). The automobile parkways appear as very linear elements that converge at the New York Botanical Garden (Site 4; NYBG) in the circuit map. The migration rate from Van Cortlandt Park (Site 6; VCN) in NW Bronx to Inwood Hill Park at the tip of Manhattan (Site 3; IP) was one of the highest BayesAss+ estimates (Table 2). Migration between these parks was largely estimated as occurring through a residential area with high tree canopy cover east of Van Cortlandt Park, and a narrow, forested park on the western coast of the Bronx (Riverdale Park; Fig. 4). The highest migration rates estimated by *Nm* and Migrate-*n* (Tables 1 and 3) were from Van Cortlandt Park into the other Bronx and Manhattan populations. Van Cortlandt Park has a larger forested area than the other parks, and large swaths of connectivity that emanate outwards in three of four directions (Fig. 4). Only the north-central Bronx was largely devoid of any predicted areas of low-resistance habitat (Fig. 4). The New York Botanical Garden (Site 4; NYBG) and Hunters Island (Site 2; HI), the central-most and northeastern-most parks in the Bronx, respectively, generally exhibited the lowest migration rates (Tables 1–3).

Estimated paths through Manhattan were very narrow, forested city parks on both the western and eastern coasts (Fig. 4). The northwestern coastal park (Fort Tryon) is largely contiguous with one of our study sites (IP, no. 3 in Fig. 1), although not coterminous with Riverside Park further south. The only clear trend in migration rates for Manhattan was that Inwood Park (Site 3; IP), situated in much greater proximity to the Bronx parks, generally exhibited higher migration rates in both directions than Central Park (Site 1; CP; Tables 1–3).

Most of the Queens Parks were distributed along the linear terminal moraine from the last glacial retreat. The landscape models predicted low to moderate connectivity along the moraine, with relative isolation for the two populations south of the moraine (Fig. 5). The highest migration rates were estimated between the two eastern-most parks, Alley Pond (Site 8; AP) and Cunningham (Site 9; CN). The circuit maps indicate a predicted forested corridor appearing as a thin, dark line (Fig. 5). Migration among other sites on the moraine was

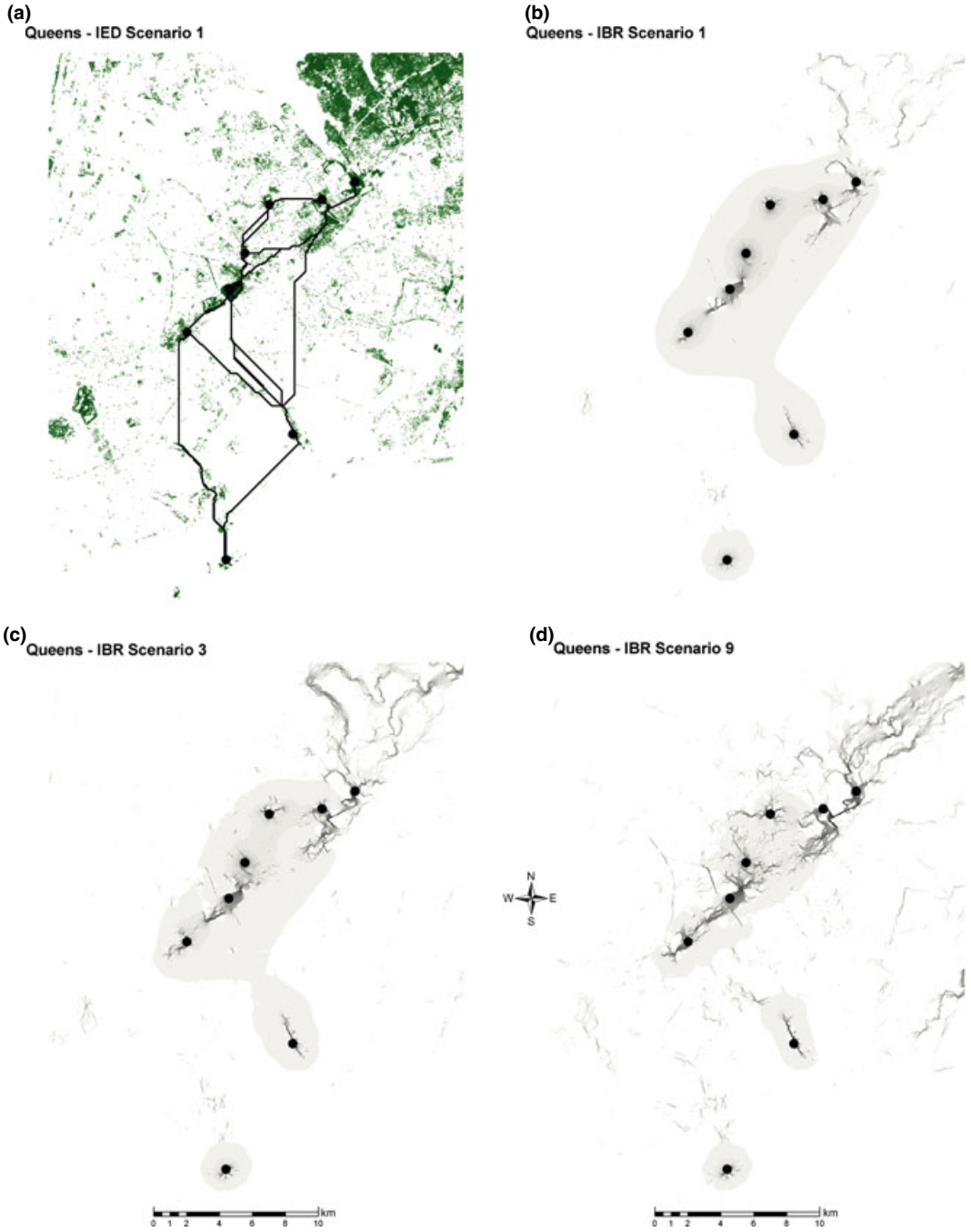

Fig. 5 Landscape models with highest partial Mantel *r* correlation coefficients for Queens populations of white-footed mice: (a) isolation-by-effective-distance model (IED; based on low resistance for 90% or more canopy cover) that was most strongly correlated with recent migration rates from BayesAss+ and (b–d) isolation-by-resistance models (IBR; based on low resistance for a minimum of 90%, 70% or 10% canopy cover, respectively) that were most strongly correlated with *Nm*, Migrate-*n* and BayesAss+ migration rates, respectively.

similarly modest, with the exception of Flushing Meadows—Willow Lake (Site 10; FM) and Ridgewood Reservoir (Site 15; RR) that exhibited generally lower rates (Tables 1–3). Although predicted paths of connectivity occur around these two sites (Fig. 5), the parks are ringed by highways.

Discussion

Urban infrastructure, connectivity models and gene flow

Connectivity models based on percentage canopy cover in NYC explained significantly more variation in gene

flow among white-footed mouse populations than isolation-by-distance (IBD) models. Significant IBD patterns were detected in NYC, likely due to relatively rare long-distance migration by *Peromyscus leucopus* (Stickel 1968). However, landscape-free IBD effects were not sufficiently strong to mask the influence of the spatial orientation of vegetation on white-footed mouse migration in NYC. Tree canopy cover models were consistently successful across three different measures of gene flow and two population clusters on isolated landmasses. Confirmation of the importance of canopy cover in two separate urban areas of NYC increases confidence in the results reported here, as species responses to landscape elements may differ between study sites (Short Bull *et al.* 2011).

The connectivity models that successfully identified pathways of migration between white-footed mouse populations in NYC included parklands not trapped for white-footed mice during this study, as well as marginal lands with no previous designation as wildlife areas, such as roadsides, cemeteries and residential areas. Although not sampled for genetic analysis, *P. leucopus* have been trapped recently in the eastern coastal Highbridge Park (J. Munshi-South, unpublished data) that appears as a migration pathway in Manhattan for both the IED and IBR analyses (Fig. 4). Close examination of connectivity between population pairs with relatively high migration rates revealed likely corridors of forest cover, such as between Alley Pond and Cunningham Parks in Queens. This corridor was the Long Island Motor Parkway from 1908 to 1938, after which time the roadway was decommissioned and converted to a bicycle/pedestrian path lined with secondary forest vegetation on both sides These pathways of migration indicate that white-footed mice can maintain limited connectivity between populations, even in one of the most urbanized locations in the world.

Many pairs of parks exhibited low migration rates despite several predicted pathways between them (i.e. Flushing Meadows—Willow Lake and Ridgewood Reservoir in Queens). The results presented here could be applied to reforestation or other urban restoration efforts that promote connectivity between green areas. NYC and many other municipal areas have recently undertaken large-scale tree-planting programs (e.g. MillionTreesNYC), although these efforts often lack a priori biological goals or rationale (Lu *et al.* 2010; McPhearson *et al.* 2011). Tree-planting or other restoration efforts would likely meet with greater success at supporting biodiversity and other ecosystem services by focusing on expanding or connecting areas that already provide ecological benefits such as connectivity. Integrating landscape ecology information from multiple species with efforts to promote appropriate stewardship and improvement of heterogeneous semi-natural areas across appropriate scales for urban conservation should be a major focus of future research (Goddard *et al.* 2010). Abundant, flexible species such as white-footed mice play important roles as both primary consumers and prey in urban forests and are often more abundant in disturbed vs. relatively pristine areas (Rytwinski & Fahrig 2007). The parameters established for gene flow and ecological connectivity of white-footed mouse populations likely do not meet thresholds for connectivity of other species, but may represent a starting point for urban management.

Human population density, urbanization and species richness are positively correlated in North America (Luck *et al.* 2004), indicating that cities and surrounding areas will be necessary components of biodiversity conservation efforts (Miller & Hobbs 2002; Sanderson & Huron 2011). Urban habitat patches are typically small and highly fragmented, but still maintain a high percentage of regional species richness (Croci *et al.* 2008); beta diversity may be especially high owing to heterogeneity in habitat quality and type between urban patches (Breuste *et al.* 2008). Few previous studies have identified urban landscape variables that powerfully predict important ecological or evolutionary processes between populations of a native species in urban habitat patches (Lada *et al.* 2008). A few studies have found that natural factors are more important than urbanization for explaining patterns of genetic structure or gene flow (Leidner & Haddad 2010; Quéméré *et al.* 2010). However, some other studies and the results found here indicate that vegetation cover or other variables (e.g. road density) are likely influencing the microevolutionary dynamics of wildlife in urban habitat fragments (Palumbi 2001; Balkenhol & Waits 2009; Simmons *et al.* 2010). Urban landscape genetics of multiple taxa with contrasting biology will greatly improve our understanding of the impacts of urbanization on native wildlife.

Comparisons of small mammal migration in multiple cities would provide an important test of urban canopy cover as a general proxy for vegetation-mediated gene flow. This study examined two clusters of populations on relatively isolated landmasses, but both clusters were located in NYC and subject to similar urbanization pressures. NYC may prove to be unique among large cities in eastern North America because of its extensive vegetation cover and replicated series of small, isolated parks in relative proximity on each of several different landmasses. Other cities in the native range of *P. leucopus* (e.g. Baltimore, Chicago and Philadelphia) tend to have less overall vegetation cover (The City of New York 2007) or are dominated by relatively few urban parks that are larger and considerably more connected

to surrounding protected areas by wide habitat corridors (e.g. Boston, Washington, D.C.). Alternatively, differences in the importance of canopy cover between NYC and other cities may be quantitative rather than qualitative, that is, other cities simply have higher gene flow facilitated by larger swaths of habitat through the urban core.

Urban landscape genetics also has an important role to play in elucidating the epidemiology of zoonotic disease in human population centres. Understanding how landscapes influence the genetic structure of parasites and pathogens directly, or through interactions between the landscape genetics of hosts and their diseases, is an important priority for urban ecologists and evolutionary biologists (Blanchong *et al.* 2008; Archie *et al.* 2009; Rees *et al.* 2009; Biek & Real 2010). White-footed mice are important hosts of the arthropod vectors of Lyme disease (*Borrelia burgdorferi*), babesiosis (*Babesia microti*) and other pathogens. However, it is currently unknown whether the spatial distribution of the vector (black-legged ticks, *Ixodes scapularis*) or pathogens are influenced by urban vegetation in the same fashion as white-footed mouse migration.

Relative success of connectivity models at explaining genetic patterns

For all but one statistic at one study site (*Nm* in Bronx & Manhattan), isolation-by-resistance (IBR) outperformed isolation-by-effective-distance (IED) models after factoring out IBD. The IED, or least-cost path, approach has been the most popular method for modelling connectivity between populations, but the calculation of one 'best' route for animal movement or gene flow through a particular set of landscape resistance values has limited utility (Sawyer *et al.* 2011). IBR has previously been shown to outperform IED because its theoretical foundations are more biologically realistic (i.e. the association between random walk times and resistance distances). IBR also accounts for heterogeneous distributions of habitat rather than assuming linear movements across continuous swaths of high-resistance landscape and effectively models multiple pathways of variable widths (McRae & Beier 2007).

Despite the advantages of IBR and the attention it has received in landscape genetics reviews (Balkenhol *et al.* 2009a; Guillot *et al.* 2009; Storfer *et al.* 2010), relatively few published studies to date have included IBR analyses. Most IBR applications have analysed broad regional patterns (McRae & Beier 2007; Lee-Yaw *et al.* 2009; Row *et al.* 2010), although the results of this study indicate that IBR can successfully predict gene flow over fine-grained scales. Zellmer & Knowles (2009) previously demonstrated the success of IBR at explaining genetic divergence between wood frog (*Rana sylvatica*) populations using the same grain and similar landscape extent as this study. The success of IBR at fine scales is important to establish because landscape genetics is most successful at identifying important landscape factors when the grain of analysis is smaller than average home ranges or lifetime movements (Anderson *et al.* 2010). One caveat is that the IBR approach assumes that the populations are continuous and gene flow could occur at any node. The populations in urban parks sampled here likely meet these criteria, but the IBR approach may not be suitable for every study system.

The nine resistance scenarios examined in this study assigned low-resistance values to consecutively lower percentages of canopy cover. Nearly all nine scenarios significantly explained variation in BayesAss+ and Migrate-*n* migration rates after factoring out IBD, with the exception of the most stringent models that assigned high resistance to all vegetated cells with less than 70–90% canopy cover (Figs 2b,d and 3b,d). Depending on the gene-flow metric and study site, the amount of variation explained in migration rates increased dramatically after 60–80% canopy cover became available as low-resistance habitat. These results demonstrate that a single, continuously distributed landscape element can produce powerful models for predicting contemporary gene flow among wild populations in urban environments.

Limitations of population genetic estimates

The bottom matrix of migration rates from BayesAss+ and Migrate-*n* were nearly equally associated with similar IBR models. The top matrix of migration rates did not exhibit IBD and was not significantly associated with any connectivity models based on canopy cover. This discrepancy indicates that immigration and emigration are not symmetric for the populations examined in this study (Tables 1–3). The causal factors for unequal migration into and out of populations in NYC are unknown. However, a recent analysis of migration rates in *Peromyscus leucopus* that also used Migrate-*n* found that emigration rates were negatively associated with the size of patches occupied by populations (Anderson & Meikle 2010). High reproductive rates in small patches could provide greater incentive to disperse out of the patch. I did not examine the influence of population density, patch size or reproductive rates, but these factors could partially explain asymmetric migration in NYC.

Surprisingly, IED and IBR models were nearly as strongly associated with *Nm* as with the migration rates from BayesAss+ and Migrate-*n*. *Nm* calculated from F_{ST} is confounded with effective population size and

reflects average, symmetric migration in both directions between populations, in contrast to the Migrate-*n* and BayesAss+ estimates that were migration in one direction between populations. Calculating *Nm* from F_{ST} is fraught with error (Whitlock & McCauley 1999) because F_{ST}-based migration typically assumes that populations have equal migration rates, random migration between populations (i.e. no geographic structure), zero mutations (an unlikely characteristic of microsatellite loci) and migration–drift equilibrium. Migration estimated from coalescent-based and nonequilibrium methods does not suffer as severely from violation of these assumptions, and uncertainty in these estimates can be assessed using confidence intervals. However, the connectivity models generated here were significantly associated with all three types of migration estimate, suggesting that IBR models are robust to the choice of gene-flow estimator. Alternatively, the populations sampled in this study may not have seriously violated the assumptions of F_{ST}-based migration calculations, leading to *Nm* estimates that accurately reflected the variation in migration between populations. Additionally, even though *Nm* is averaged in both directions between populations, the spatial signal from migration in one direction may have been strong enough to not be fully masked in the *Nm* estimates.

The Bayesian coalescent approach implemented in Migrate-*n* may also be influenced by deviation from equilibrium assumptions. However, the similar success at IBR models in explaining coalescent-based and nonequilibrium assignment–based migration estimates suggests that such violations were not severe. White-footed mouse populations in NYC have been fragmented for the last few hundred generations. Thus, they are likely close to migration–drift equilibrium, especially given the success of equilibrium-based methods at identifying unique evolutionary clusters (Munshi-South & Kharchenko 2010). Migrate-*n* generally produced more nonzero estimates of pairwise migration than BayesAss+. This pattern could be explained by reduced contemporary connectivity because of degradation of natural areas in NYC. Much of NYC was rapidly urbanized over a few decades in the early 20th century as development tracked the construction of subways, especially outside lower Manhattan; many of the city's fragmented green spaces were gazetted as city parks during the same period (Caro 1974). Thus, it seems unlikely that white-footed mouse migration was substantially higher at some period in the last century than contemporary migration. Historical maps of canopy cover are not readily available, but if collated from historical sources, then the influence of past landcover on longer-term migration rates could be investigated (Zellmer & Knowles 2009).

Migrate-*n* is known to overestimate migration when divergence times are not substantially larger than N_E within subpopulations. The influence of incomplete lineage sorting and resultant similarity of the subpopulations cannot be easily disentangled from migration in these cases, leading to inflated estimates (Edwards & Beerli 2000). White-footed mouse populations in NYC are generally large and genetically variable (Munshi-South & Kharchenko 2010), and thus potentially subject to this inflation. However, the directionality of migration rates is preserved despite recent divergence times and large N_E (P. Beerli, personal communication), which may partially explain why the same IBR models were significantly associated with migration estimates from both BayesAss+ and Migrate-*n*.

Limitations of landscape modelling approach

Although the models used in this study successfully explained variation in gene flow, there were limitations of the landscape modelling approach. Beier *et al.* (2008) identified sixteen key questions for studies of connectivity among wild populations, covering aspects of sampling design, analysis of landscape resistance and implementation of results for conservation projects. The most important questions for this study are the influence of the spatial extent of analysis, choice of landscape elements and choice of resistance values. The spatial extent considered in a connectivity study influences the particular landscape configurations that are included in the downstream analyses (Anderson *et al.* 2010). Examining too small of a geographic area can thus erroneously exclude areas of the landscape that have a large influence on gene-flow patterns. I protected against this danger by including large counties adjacent to NYC in the analysis, and all important pathways of connectivity detected by the IED and IBR were wholly contained within the sampled landscape by a large margin.

Per cent canopy cover was chosen as the most influential variable for connectivity because the nonvegetated landscape in NYC consists almost entirely of impermeable surfaces, high human population density and water. Furthermore, extensive trapping records throughout NYC indicate that white-footed mice occur in nearly all forested patches but are absent from nonvegetated areas (Ekernas & Mertes 2007; Puth & Burns 2009; Munshi-South & Kharchenko 2010). Nearly all parks also have roadways as boundaries, and thus there was little landscape variation outside a measure of vegetation that would have biological meaning for small mammal movement. Tree canopy cover does have limitations as a measure of vegetation, however, as it may not account for grassy areas with no shrubs or trees

(especially mowed lawns), and does not account for human management practices underneath the canopy. Some information may also have been lost by using categorical bins of per cent canopy cover rather than continuous percentages, but both the landscape and genetic data were likely too coarse to resolve more subtle gradient patterns. Canopy cover from the National Land Cover Database is calculated at 30-m resolution (Homer *et al.* 2004), which is fine-grained enough to capture habitat use (Stickel 1968) and migration (Anderson & Meikle 2010) of white-footed mice. Finer-scale data sets, such as categorical landcover in NYC at 1-m resolution (Myeong *et al.* 2001), are increasingly available and may enhance the explanatory value of resistance models in future studies.

Choice of resistance values for landscape genetic analyses will necessarily be subjective when data on species movements through different landcover elements are lacking (Beier *et al.* 2008). High-contrast resistance values (1 vs. 10 000) were used in this study to identify specific levels of canopy cover that would dramatically increase the correlation with gene flow when included as low-resistance habitat. Landscape resistance values used here were chosen independently of the genetic estimates of differentiation or migration. Given the very high correlation between IBR models and recent gene flow, one can conclude that the resistance scenarios were biologically realistic. However, connectivity between urban white-footed mice may decrease more gradually with canopy cover than was estimated in this study. Long-term mark–recapture or telemetry studies over a range of canopy cover would require considerable effort, but such data would provide valuable confirmation before translating landscape genetic results into the construction of biological corridors, reforestation or other conservation activities (Beier *et al.* 2008; Lowe & Allendorf 2010).

Concerns have recently been raised that population-based, rather than individual-based, landscape genetic analyses are prone to erroneous inference because of unrecognized internal structure of populations (Cushman & Landguth 2010; Segelbacher *et al.* 2010). Several independent analyses that did not assume a priori population structure were conducted to establish the evolutionary uniqueness of the populations analysed here (Munshi-South & Kharchenko 2010). Individual-based pairwise analyses may perform poorly if the genetic data are highly autocorrelated as a result of sampling multiple individuals from the same (sub)populations. Given that many estimates of recent migration between *Peromyscus leucopus* populations in NYC were indistinguishable from zero (Table 3) and most sampling sites were very small habitat patches (i.e. city parks), such autocorrelation within populations would likely be a problem for individual-based analysis of these data. Furthermore, migration rates are genetic properties of populations (Marko & Hart 2011). Individual-based approaches typically examine pairwise relatedness or genetic distance between individuals (Coulon *et al.* 2004), and while related, these statistics are not synonymous with gene flow.

Partial Mantel tests have often been used in landscape genetic studies to control for IBD between populations (Storfer *et al.* 2010) and thus identify connectivity models that are significant beyond their correlation with Euclidean distance. Some authors have criticized these tests for ascribing significance to connectivity metrics that are merely correlated with migration but not truly influential on their own (Balkenhol *et al.* 2009b). However, partial Mantel tests can be successful when alternative models are tested against each other as was done here to identify the superiority of IBR to IED/IBD models (Cushman & Landguth 2010). In general, partial Mantel tests perform as well as regression and approximate Bayesian computation techniques, but with the caveats that important landscape elements must strongly influence gene flow and have very different permeability to migration than other elements (Jaquiéry *et al.* 2011). Partial Mantel tests were powerful at identifying levels of canopy cover that impeded or facilitated gene flow in a relatively simple urban landscape, although the active interest in developing new statistical frameworks for landscape genetics may produce superior approaches in the future.

Acknowledgements

This work was funded by the National Science Foundation (DEB 0817259) and two grants from the Professional Staff Congress-CUNY. Five anonymous reviewers provided very helpful comments in revising the manuscript. I thank the National Park Service, New York State Department of Environmental Conservation, Natural Resources Group of the NYC Dept. of Parks and Recreation, the Central Park Conservancy, Regina Alvarez, Ellen Pehek and Jessica Arcate Schuler for access to NYC study sites. I thank David Burg, Catherine Burns, Paolo Cocco, Jonathan Grindley, Stephen Harris, Kerstin Kalchmayr, Olga Lavinda, Luca Pozzi and Miguel Rivera for their invaluable help collecting samples in the field. Katerina Kharchenko worked tirelessly in the laboratory to generate the genotypic data for this project. Mary Blair provided ArcGIS scripts and much advice on spatial connectivity modelling.

References

Anderson CS, Meikle DB (2010) Genetic estimates of immigration and emigration rates in relation to population density and forest patch area in *Peromyscus leucopus*. *Conservation Genetics*, **11**, 1593–1605.

Anderson C, Epperson BK, Fortin MJ *et al.* (2010) Considering spatial and temporal scale in landscape-genetic studies of gene flow. *Molecular Ecology*, **19**, 3565–3575.

Archie EA, Luikart G, Ezenwa VO (2009) Infecting epidemiology with genetics: a new frontier in disease ecology. *Trends in Ecology & Evolution*, **24**, 21–30.

Balkenhol N, Waits L (2009) Molecular road ecology: exploring the potential of genetics for investigating transportation impacts on wildlife. *Molecular Ecology*, **18**, 4151–4164.

Balkenhol N, Gugerli F, Cushman SA *et al.* (2009a) Identifying future research needs in landscape genetics: where to from here? *Landscape Ecology*, **24**, 455–463.

Balkenhol N, Waits LP, Dezzani RJ (2009b) Statistical approaches in landscape genetics: an evaluation of methods for linking landscape and genetic data. *Ecography*, **32**, 818–830.

Beerli P (2006) Comparison of Bayesian and maximum likelihood inference of population genetic parameters. *Bioinformatics*, **22**, 341–345.

Beerli P, Felsenstein J (2001) Maximum likelihood estimation of a migration matrix and effective population sizes in n subpopulations by using a coalescent approach. *Proceedings of the National Academy of Sciences of the United States of America*, **98**, 4563–4568.

Beier P, Majka DR, Spencer WD (2008) Forks in the road: choices in procedures for designing wildland linkages. *Conservation Biology*, **22**, 836–851.

Biek R, Real LA (2010) The landscape genetics of infectious disease emergence and spread. *Molecular Ecology*, **19**, 3515–3531.

Bjorklund M, Ruiz I, Senar J (2010) Genetic differentiation in the urban habitat: the great tits (*Parus major*) of the parks of Barcelona city. *Biological Journal of the Linnean Society*, **99**, 9–19.

Blanchong JA, Samuel MD, Scribner KT, Weckworth BV, Langenberg J, Filcek KB (2008) Landscape genetics and the spatial distribution of chronic wasting disease. *Biology Letters*, **4**, 130–133.

City of New York (2007) *PlaNYC: A Greener, Greater New York*. The City of New York, New York, New York.

Bohonak AJ (1999) Dispersal, gene flow, and population structure. *The Quarterly Review of Biology*, **74**, 21–45.

Breuste J, Niemelä J, Snep R (2008) Applying landscape ecological principles in urban environments. *Landscape Ecology*, **23**, 1139–1142.

Broquet T, Ray N, Petit E, Fryxell JM, Burel F (2006) Genetic isolation by distance and landscape connectivity in the American marten (*Martes americana*). *Landscape Ecology*, **21**, 877–889.

Caro RA (1974) *The Power Broker: Robert Moses and the Fall of New York*. Alfred A Knopf, New York, New York.

Coulon A, Cosson JF, Angibault JM *et al.* (2004) Landscape connectivity influences gene flow in a roe deer population inhabiting a fragmented landscape: an individual–based approach. *Molecular Ecology*, **13**, 2841–2850.

Croci S, Butet A, Georges A, Aguejdad R, Clergeau P (2008) Small urban woodlands as biodiversity conservation hot-spots: a multi-taxon approach. *Landscape Ecology*, **23**, 1171–1186.

Cushman SA, Landguth EL (2010) Spurious correlations and inference in landscape genetics. *Molecular Ecology*, **19**, 3592–3602.

Delaney KS, Riley SPD, Fisher RN (2010) A rapid, strong, and convergent genetic response to urban habitat fragmentation in four divergent and widespread vertebrates. *PLoS ONE*, **5**, e12767.

Edwards SV, Beerli P (2000) Gene divergence, population divergence, and the variance in coalescence time in phylogeographic studies. *Evolution*, **54**, 1839–1854.

Ekernas LS, Mertes KJ (2007) The influence of urbanization, patch size, and habitat type on small mammal communities in the New York metropolitan region: a preliminary report. *Transactions of the Linnaean Society of New York*, **10**, 239–264.

Epps CW, Wehausen JD, Bleich VC, Torres SG, Brashares JS (2007) Optimizing dispersal and corridor models using landscape genetics. *Journal of Applied Ecology*, **44**, 714–724.

Etherington TR (2011) Python based GIS tools for landscape genetics: visualising genetic relatedness and measuring landscape connectivity. *Methods in Ecology and Evolution*, **2**, 52–55.

Fahrig L (2003) Effects of habitat fragmentation on biodiversity. *Annual Review of Ecology, Evolution, and Systematics*, **34**, 487–515.

Faubet P, Waples RS, Gaggiotti OE (2007) Evaluating the performance of a multilocus Bayesian method for the estimation of migration rates. *Molecular Ecology*, **16**, 1149–1166.

Frankham R (2010) Challenges and opportunities of genetic approaches to biological conservation. *Biological Conservation*, **143**, 1919–1927.

Gaines M, Diffendorfer J, Tamarin R, Whittam T (1997) The effects of habitat fragmentation on the genetic structure of small mammal populations. *Journal of Heredity*, **88**, 294–304.

Garant D, Forde SE, Hendry AP (2007) The multifarious effects of dispersal and gene flow on contemporary adaptation. *Functional Ecology*, **21**, 434–443.

Gardner-Santana L, Norris D, Fornadel C, Hinson E, Klein SL, Glass GE (2009) Commensal ecology, urban landscapes, and their influence on the genetic characteristics of city-dwelling Norway rats (*Rattus norvegicus*). *Molecular Ecology*, **18**, 2766–2778.

Goddard MA, Dougill AJ, Benton TG (2010) Scaling up from gardens: biodiversity conservation in urban environments. *Trends in Ecology & Evolution*, **25**, 90–98.

Goslee SC, Urban DL (2007) The ecodist package for dissimilarity-based analysis of ecological data. *Journal of Statistical Software*, **22**, 1–19.

Guillot G, Leblois R, Coulon A, Frantz AC (2009) Statistical methods in spatial genetics. *Molecular Ecology*, **18**, 4734–4756.

Hapeman P, Latch EK, Fike JA, Rhodes OE, Kilpatrick CW (2011) Landscape genetics of fishers (*Martes pennanti*) in the northeast: dispersal barriers and historical influences. *Journal of Heredity*, **102**, 251–259.

Holderegger R, Wagner HH (2008) Landscape genetics. *BioScience*, **58**, 199–207.

Homer C, Huang C, Yang L, Wylie B *et al.* (2004) Development of a 2001 national landcover database for the United States. *Photogrammetric Engineering and Remote Sensing*, **70**, 829–840.

Horenstein S (2007) Inwood Hill and Isham parks: geology, geography, and history. *Transactions of the Linnaean Society of New York*, **10**, 1–54.

Jaquiéry J, Broquet T, Hirzel AH, Yearsley J, Perrin N (2011) Inferring landscape effects on dispersal from genetic distances: how far can we go? *Molecular Ecology*, **20**, 692–705.

Jenkins DG, Carey M, Czerniewska J *et al.* (2010) A meta-analysis of isolation by distance: relic or reference standard for landscape genetics? *Ecography*, **33**, 315–320.

Keyghobadi N (2007) The genetic implications of habitat fragmentation for animals. *Canadian Journal of Zoology*, **85**, 1049–1064.

Krohne D, Hoch G (1999) Demography of *Peromyscus leucopus* populations on habitat patches: the role of dispersal. *Canadian Journal of Zoology*, **77**, 1247–1253.

Lada H, Thomson J, Mac Nally R, Taylor A (2008) Impacts of massive landscape change on a carnivorous marsupial in south-eastern Australia: inferences from landscape genetics analysis. *Journal of Applied Ecology*, **45**, 1732–1741.

Lee-Yaw JA, Davidson A, McRae BH, Green DM (2009) Do landscape processes predict phylogeographic patterns in the wood frog? *Molecular Ecology*, **18**, 1863–1874.

Leidner AK, Haddad NM (2010) Natural, not urban, barriers define population structure for a coastal endemic butterfly. *Conservation Genetics*, **11**, 2311–2320.

Lowe WH, Allendorf FW (2010) What can genetics tell us about population connectivity? *Molecular Ecology*, **19**, 3038–3051.

Lu JWT, Shane M, Svendsen E (2010) *MillonTreesNYC, Green Infrastructure, and Urban Ecology: Building a Research Agenda*. City of New York Parks & Recreation, New York, New York.

Luck GW, Ricketts TH, Daily GC, Imhoff M (2004) Alleviating spatial conflict between people and biodiversity. *Proceedings of the National Academy of Sciences of the United States of America*, **101**, 182–186.

Maier T (2002) Long-distance movements by female White-footed Mice, *Peromyscus leucopus*, in extensive mixed-wood forest. *Canadian Field-Naturalist*, **116**, 108–111.

Manel S, Schwartz MK, Luikart G, Taberlet P (2003) Landscape genetics: combining landscape ecology and population genetics. *Trends in Ecology and Evolution*, **18**, 189–197.

Marko PB, Hart MW (2011) The complex analytical landscape of gene flow inference. *Trends in Ecology & Evolution*, **26**, 448–456.

McKinney ML (2006) Urbanization as a major cause of biotic homogenization. *Biological Conservation*, **127**, 247–260.

McPhearson PT, Feller M, Felson A *et al.* (2011) Assessing the effects of the urban forest restoration effort of MillionTreesNYC on the structure and functioning of New York city ecosystems. *Cities and the Environment*, **3**, 1–21.

McRae BH (2006) Isolation by resistance. *Evolution*, **60**, 1551–1561.

McRae BH, Beier P (2007) Circuit theory predicts gene flow in plant and animal populations. *PNAS*, **104**, 19885–19890.

Mech S, Hallett J (2001) Evaluating the effectiveness of corridors: a genetic approach. *Conservation Biology*, **15**, 467–474.

Miller JR, Hobbs RJ (2002) Conservation where people live and work. *Conservation Biology*, **16**, 330–337.

Munshi-South J, Kharchenko K (2010) Rapid, pervasive genetic differentiation of urban white-footed mouse (*Peromyscus leucopus*) populations in New York City. *Molecular Ecology*, **19**, 4242–4254.

Myeong S, Nowak DJ, Hopkins PF, Brock RH (2001) Urban cover mapping using digital, high-spatial resolution aerial imagery. *Urban Ecosystems*, **5**, 243–256.

Nagy C, Bardwell K, Rockwell RF, Christie R, Weckel M (in press) Validation of a citizen science-based model of site occupancy for eastern screech owls with systematic data in suburban New York and connecticut. *Northeastern Naturalist*, in press.

Noël S, Lapointe F-J (2010) Urban conservation genetics: study of a terrestrial salamander in the city. *Biological Conservation*, **143**, 2823–2831.

Nupp T, Swihart R (1996) Effect of forest patch area on population attributes of white-footed mice (*Peromyscus leucopus*) in fragmented landscapes. *Canadian Journal of Zoology*, **74**, 467–472.

Palumbi S (2001) Humans as the world's greatest evolutionary force. *Science*, **293**, 1786–1790.

Peakall ROD, Smouse PE (2006) GENALEX 6: genetic analysis in Excel. Population genetic software for teaching and research. *Molecular Ecology Notes*, **6**, 288–295.

Pearse D, Crandall K (2004) Beyond F_{st}: analysis of population genetic data for conservation. *Conservation Genetics*, **5**, 585–602.

Pease KM, Freedman AH, Pollinger JP *et al.* (2009) Landscape genetics of California mule deer (*Odocoileus hemionus*): the roles of ecological and historical factors in generating differentiation. *Molecular Ecology*, **18**, 1848–1862.

Pećarević M, Danoff-Burg J, Dunn RR (2010) Biodiversity on broadway – enigmatic diversity of the societies of ants (Formicidae) on the streets of New York City. *PLoS ONE*, **5**, e13222.

Perez-Espona S, Perez-Barberia F, McLeod JE, Jiggins CD, Gordon IJ, Pemberton JM (2008) Landscape features affect gene flow of Scottish Highland red deer (*Cervus elaphus*). *Molecular Ecology*, **17**, 981–996.

Puth LM, Burns CE (2009) New York's nature: a review of the status and trends in species richness across the metropolitan region. *Diversity and Distributions*, **15**, 12–21.

Quéméré E, Crouau-Roy B, Rabarivola C, Louis Jr EE, Chikhi L (2010) Landscape genetics of an endangered lemur (*Propithecus tattersalli*) within its entire fragmented range. *Molecular Ecology*, **19**, 1606–1621.

R Development Core Team (2008) *R: A Language and Environment for Statistical Computing*. R Foundation for Statistical Computing, Vienna, Austria.

Rayfield B, Fortin M, Fall A (2010) The sensitivity of least-cost habitat graphs to relative cost surface values. *Landscape Ecology*, **25**, 519–532.

Rees EE, Pond BA, Cullingham CI *et al.* (2009) Landscape modelling spatial bottlenecks: implications for raccoon rabies disease spread. *Biology Letters*, **5**, 387–390.

Ricketts T (2001) The matrix matters: effective isolation in fragmented landscapes. *American Naturalist*, **158**, 87–99.

Row JR, Blouin-Demers G, Lougheed SC (2010) Habitat distribution influences dispersal and fine-scale genetic population structure of eastern fox snakes (*Mintonius gloydi*) across a fragmented landscape. *Molecular Ecology*, **19**, 5157–5171.

Rytwinski T, Fahrig L (2007) Effect of road density on abundance of white-footed mice. *Landscape Ecology*, **22**, 1501–1512.

Sanderson EW, Huron A (2011) Conservation in the city. *Conservation Biology*, **25**, 421–423.

Sawyer SC, Epps CW, Brashares JS (2011) Placing linkages among fragmented habitats: do least-cost models reflect how animals use landscapes? *Journal of Applied Ecology*, **48**, 668–678.

Schoener A, Schoener TW (1984) Experiments on dispersal: short-term floatation of insular anoles, with a review of similar abilities in other terrestrial animals. *Oecologia*, **63**, 289–294.

Segelbacher G, Cushman S, Epperson B *et al.* (2010) Applications of landscape genetics in conservation biology: concepts and challenges. *Conservation Genetics*, **11**, 375–385.

Shah VB, McRae BH (2008) Circuitscape: a tool for landscape ecology. *Proceedings of the 7th Python in Science Conference*. pp. 62–66.

Short Bull RA, Cushman SA, Mace R *et al.* (2011) Why replication is important in landscape genetics: American black bear in the Rocky mountains. *Molecular Ecology*, **20**, 1092–1107.

Simmons JM, Sunnucks P, Taylor AC, van der Ree R (2010) Beyond roadkill, radiotracking, recapture and F_{ST}—a review of some genetic methods to improve understanding of the influence of roads on wildlife. *Ecology and Society*, **15**, 9.

Stickel LF (1968) Home range and travels. *Biology of Peromyscus (Rodentia)*. The American Society of Mammalogists, Stillwater, OK. pp. 373–411. Special Publication No. 2.

Storfer A, Murphy MA, Spear SF, Holderegger R, Waits LP (2010) Landscape genetics: where are we now? *Molecular ecology*, **19**, 3496–3514.

Varvio SL, Chakraborty R, Nei M (1986) Genetic variation in subdivided populations and conservation genetics. *Heredity*, **57**, 189–198.

Waples RS, Gaggiotti O (2006) What is a population? An empirical evaluation of some genetic methods for identifying the number of gene pools and their degree of connectivity *Molecular Ecology*, **15**, 1419–1440.

Whitlock MC, McCauley DE (1999) Indirect measures of gene flow and migration: FST not equal to 1/(4Nm + 1). *Heredity*, **82**(Pt 2), 117–125.

Wilson G, Rannala B (2003) Bayesian inference of recent migration rates using multilocus genotypes. *Genetics*, **163**, 1177–1191.

Zellmer AJ, Knowles LL (2009) Disentangling the effects of historic vs. contemporary landscape structure on population genetic divergence. *Molecular Ecology*, **18**, 3593–3602.

J.M.-S. is an assistant professor of biology at Baruch College and the Graduate Center of the City University of New York (CUNY). He is broadly interested in the evolutionary consequences of human-driven landscape change for wildlife populations. His laboratory is currently investigating neutral and adaptive evolution among vertebrate populations in New York City using population genomic approaches.

Data accessibility

The microsatellite genotypes, spatial coordinates of sampled populations, and nine resistance grids used to calculate both effective and resistance distances are available on the Dryad digital repository (doi: 10.5061/dryad.7gh65757).

Supporting information

Table S1 Euclidean geographic distances (km; above diagonal) and Slatkin's linearized F_{ST} (below diagonal) estimated between each pair of populations in the Bronx & Manhattan (top) and Queens (bottom). Sample sizes (*N*) appear next to each population in the first column.

Table S2 95% confidence intervals for recent migration rates from Table 2 estimated between each pair of populations in the Bronx & Manhattan (top) and Queens (bottom) using BayesAss+ 1.3. Values above the diagonal are migration rates from the populations in the horizontal row into the populations in the vertical column, and values below the diagonal are migration rates from the populations in the vertical column into the populations in the horizontal row.

Table S3 Median values and 95% confidence intervals for unidirectional migration rates, M (m/μ), estimated between each pair of populations in the Bronx & Manhattan (top) and Queens (bottom) using Migrate-*n* 3.2.1. Values are presented for each of the five independent runs of Migrate-*n*.

Table S4 Resistance values assigned to 30×30 m landscape cells in each of nine different resistance scenarios based on percentage of tree canopy cover.

Table S5 Simple Mantel correlation coefficients, *P*-values, and 95% confidence intervals calculated for all nine IED and IBR models using *Nm*, recent migration rates from BayesAss+, and migration rates from Migrate-*n* as measures of gene flow.